Artificial atom and quantum terahertz response in carbon nanotube quantum dots

2008 J. Phys.: Condens. Matter 20 454203

(http://iopscience.iop.org/0953-8984/20/45/454203)

J. Phys.: Condens. Matter **20** (2008) 454203 (5pp) doi:10.1088/0953-8984/20/45/454203

Artificial atom and quantum terahertz response in carbon nanotube quantum dots

K Ishibashi, S Moriyama[1], T Fuse[2], Y Kawano, S Toyokawa and T Yamaguchi

Advanced Device Laboratory, RIKEN, 2-1, Hirosawa, Wako, Saitama 351-0198, Japan

E-mail: e-mail: kishiba@riken.jp

Received 2 June 2008, in final form 22 July 2008
Published 23 October 2008
Online at stacks.iop.org/JPhysCM/20/454203

Abstract

Artificial atom behaviours have been observed in single-wall carbon nanotube (SWCNT) quantum dots (QDs). Two-electron shell structures and the Zeeman splitting of single-particle states were revealed in single-electron transport measurements in low temperatures. To demonstrate that the charging energy of the dot lies in a terahertz (THz) range, the THz photon-assisted tunnelling was tested, and was really observed as a satellite Coulomb peak. Some satellite peaks moved as a frequency was changed, but other peaks did not move. We give possible models to explain the existence of two different satellite peaks.

(Some figures in this article are in colour only in the electronic version)

1. Introduction

Single quantum dots (QDs) have been realized in an individual single-wall carbon nanotube (SWCNT) simply by depositing metallic contacts on top of it [1, 2] and its transport properties have been measured [1–3]. These measurements revealed that the SWCNT-QDs behave as an artificial atom with shells that accommodate four or two electrons [4–6]. One unique feature in the SWCNT-QD is the fact that the shell structure is observable even with many electrons in the QD, which is in striking contrast to popular semiconductor QDs where the shell structures are observable only when the number of electrons are small, typically less than ten [7]. Another unique feature is that energy scales associated with the QD, namely the single-electron charging energy (E_c) and the level spacing (ΔE), are larger by an order than those in the semiconductor QDs. They can be in the millimetre to terahertz (THz) range, depending on the distance between the contacts. Due to this fact, a strong interaction between SWCNT-QD and THz wave is expected [8]. The larger energy scales of the QDs mean the possible observation of the single-electron effects at higher temperatures, which is practically important for the single-electron devices with SWCNTs [9]. The possible observation of artificial atom characteristics may be advantageous for the spin-based quantum bit (qubit) [10, 11]. In this paper, we review artificial atom characteristics of SWCNT-QDs and demonstrate their quantum response to THz waves.

[1] Present address: National Institute of Materials Science (NIMS), 1-1, Namiki, Tsukuba, Ibaraki 305-0044, Japan.

[2] Present address: Kavli Institute of Nanoscience, Delft University of Technology, Lorentzweg 1, 2628CJ Delft, The Netherlands.

2. Quantum dot and artificial atom

The quantum dot is considered as an artificial atom, in that it contains electrons in a small space. QDs have been fabricated in a GaAs/AlGaAs two-dimensional electron gas, and recently in carbon nanotubes. The artificial atom behaviours were first observed in the vertical QD made from GaAs-based heterostructures, and the shell structures were observed when the number of electrons was small [7]. Recently, the artificial atom behaviours have been observed in SWCNT-QDs in their transport measurements at low temperatures [4, 5]. Figure 1(a) shows the scanning electron microscope image of the SWCNT-QD. The single QD is formed in between the two metallic contacts. In figure 1(b), the Coulomb oscillations are shown and the addition energy (E_{add}), which is obtained from the peak spacings, is shown in figure 1(d). Each peak is well fitted by the theoretical expression [12]. In the orthodox model of Coulomb oscillations, which ignores the effect of ΔE, the peak spacing

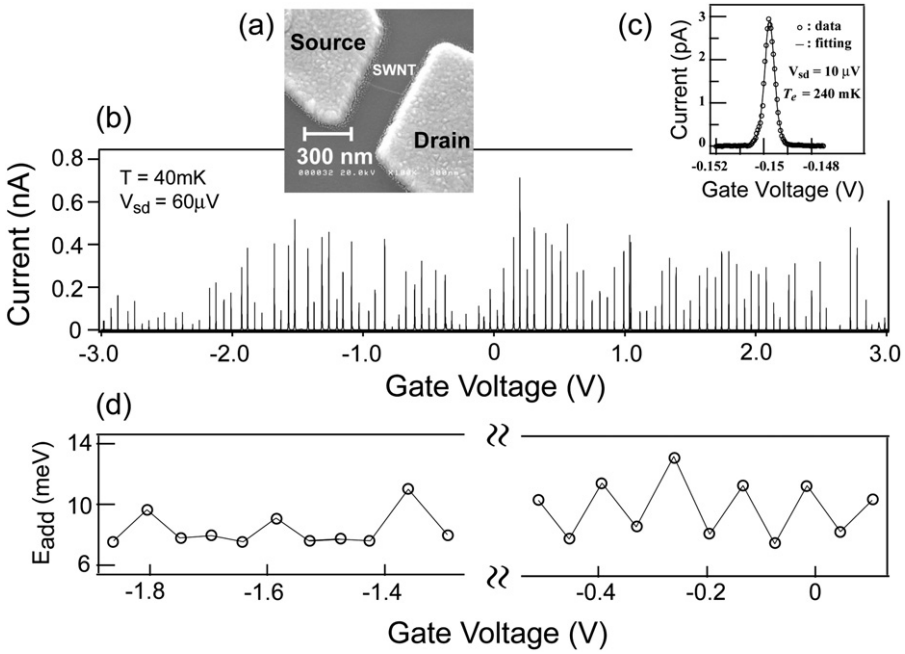

Figure 1. (a) Scanning electron microscope image of the sample. (b) Current as a function of the gate voltage (Coulomb oscillations). (c) Blow-up shape of a Coulomb peak fitted with a theoretical curve. (d) Addition energy as a function of the gate voltage in two different regions.

is constant, independent of the gate voltage or equivalently the number of electrons [13]. However, as seen in figure 1(d), $E_{\rm add}$ is not constant and has a four-electron periodicity in one gate voltage range and a two-electron periodicity in another gate voltage range. The four-electron periodicity arises from the existence of two bands near the Fermi energy in addition to the spin degeneracy. When the band degeneracy is lifted by some means, such as defects or some other imperfections, which may destroy crystal symmetry, the spin degeneracy still remains, resulting in the two-electron periodicity [14].

Figure 2(a) shows Coulomb diamonds with the two-electron periodicity. The diamonds with a large and small size appear alternately, which is the even–odd effect [15]. In the larger diamonds, the number of electrons is even and, in the smaller diamonds, it is odd. The Coulomb peaks that appear at the gate voltages where two diamonds meet move linearly as the magnetic field is increased. The peak indicated by the left circle moves in a left direction, while the peak indicated by the right circle moves in a right direction. The mechanism for the effect is understood by a schematic model shown in figure 3. The situation in figure 3(a) corresponds to the left peak. In this case, the new electron indicated by the red arrow occupies the lower level of the Zeeman-split two levels as the gate voltage is increased. In figure 3(b), the situation which corresponds to the right peak, the new electron indicated by the red arrow occupies the upper level of the Zeeman-split two levels. The slope of the peak shift, which gives the g factor, is very close to 2. The important implication is that the total spin is $1/2$ when the number of electrons is odd, a situation for the spin qubit.

In the SWCNT-QD, a simple shell filling occurs, meaning that an electron occupies successively from the lower levels with an opposite spin in the same level. This is also because of the unique energy scales of the QD. The interaction energies, such as on-site interaction energy and exchange interaction energy, are of the order of 0.1 meV which is much larger than ΔE [5]. A unique feature of the system, as compared with semiconductor quantum dots, is that the shell structures are observable even with many electrons in the dot. This is due to the degree of degeneracy of the single-particle levels of the SWCNT-QD that does not depend on the levels and is always four or two, depending on the existence of the band degeneracy. In contrast to that, the degree of the degeneracy increases as the quantum number increases in the semiconductor QDs with a two-dimensional parabolic potential. This fact may make the observation of shell structures difficult when the number of electrons is increased.

3. THz photon-assisted tunnelling

The fact that the energy scales associated with the SWCNT-QDs exist in a THz range makes us expect a quantum response of the QD to the THz wave, and the effect could be applied for high sensitivity detectors with spectroscopic capability. To test the idea, we have performed experiments where the single-electron transport was measured at $T = 1.5$ K under THz wave irradiation with different frequencies and powers [16]. We have observed two kinds of satellite peaks with different behaviours, one which moved as the THz frequency was changed (type-1 peak) and the other which did not move as the THz frequency was changed (type-2 peak). The results for the type-1 peak are shown in figure 4. As seen in figure 4(a), the new satellite peaks, indicated by arrows, are observed on the right-hand side of the main Coulomb peaks

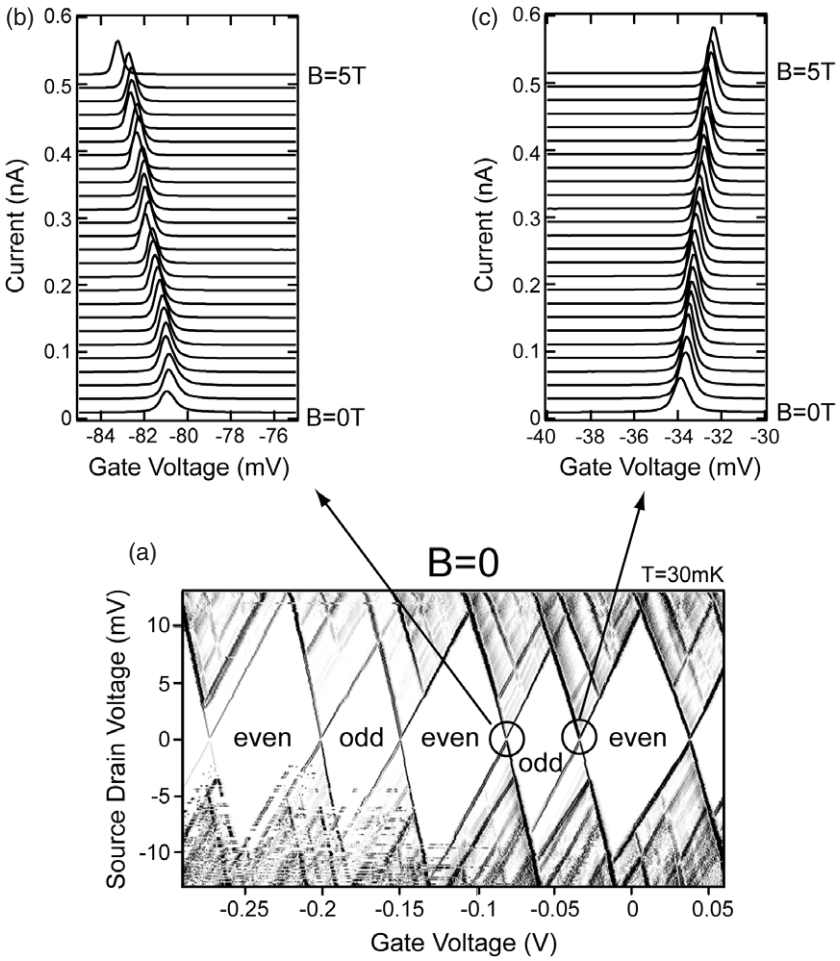

Figure 2. (a) Coulomb diamonds in the two-electron regime. (b) Coulomb peak in magnetic fields for the number of electrons increasing from even to odd. (c) Coulomb peak in magnetic fields for the number of electrons increasing from odd to even.

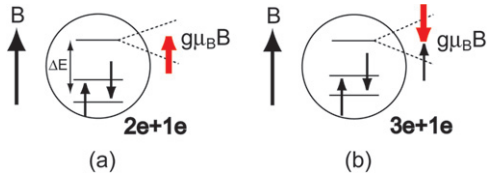

Figure 3. Schematic model of the direction of the peak shift (a) for peak (b) in figure 2 and (b) for peak (c) in figure 2.

when the THz wave is irradiated. The satellite peak position depends on the THz frequency and the peak position moves away from the main Coulomb peak as the THz frequency is increased. The distances in a gate voltage between the main Coulomb peak and the satellite peak can be converted into energy by multiplying a gate conversion factor, and are shown in figure 4(b) as a function of the applied THz frequency. It is seen that each experimental point lies on the line with a slope of 1, suggesting the photon-related origin.

The mechanism of the satellite peaks in figure 4(a) that move with frequencies is shown in figure 6(a). The QD is in the Coulomb blockade regime without THz irradiation and contains N electrons in it. However, when the THz wave is irradiated, an electron in the QD can absorb the THz photon to tunnel out in the drain electrode on the right (the electron sitting on the green level in figure 6(a)). This is the THz photon-assisted tunnelling (THz-PAT). If an electron comes in the same level in the QD from the source electrode in the left, the process contributes to the current. It may be possible for an electron from the drain electrode to come in the level in the QD: then the process does not contribute to the current. In any case, an electron in the QD may absorb the THz photon to contribute to the current. It should be noted that, since the tunnelling electron comes in the bias window set by V_{sd} in the drain electrode, the process forms the current peak.

There should also be a type-1 peak on the left-hand side of the main peak, which also moves as the THz frequency is changed. In this case, an electron in the bias window in the source would tunnel into the upper empty level by absorbing a THz photon. To be consistent with figure 6(a), the upper level should be the Nth electron level because there are $N-1$ electrons in the QD at the gate voltage without THz irradiation. Experimentally, however, we have not seen the photon peaks of this type that should appear on the left-hand side of the main peak. The reason for this is not clear, but one possibility is that the tunnel barrier is not high enough in practice to form the upper level. In the previous work, the effective height of the

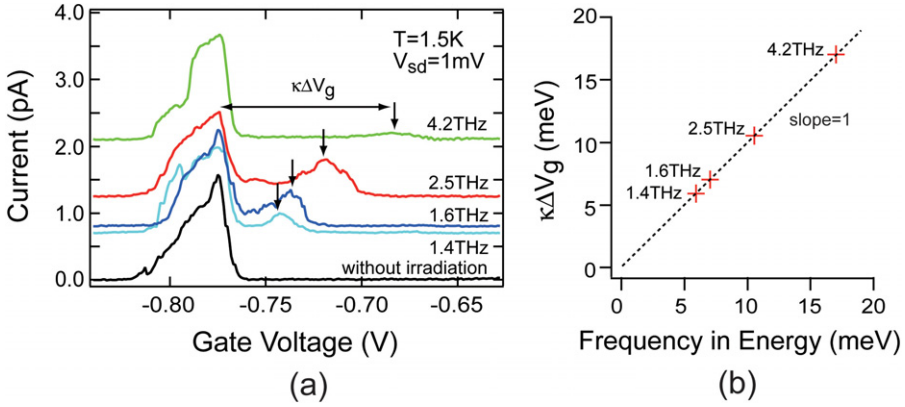

Figure 4. (a) Coulomb peaks with and without different THz frequencies. The satellite peaks indicated by the arrows are photon-assisted tunnelling peaks. (b) The energy difference between the main Coulomb peak and the satellite peak as a function of the frequency in energy.

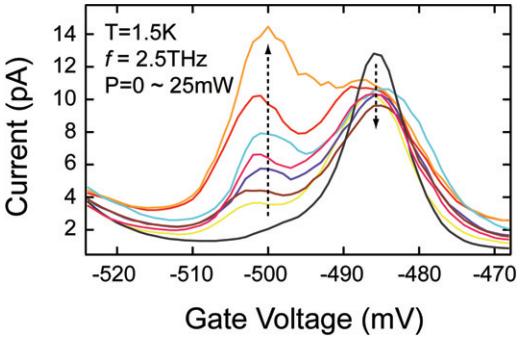

Figure 5. Satellite peak that does not change its position as the THz frequency is changed. The figure shows the main Coulomb peak and the satellite peak with different THz powers.

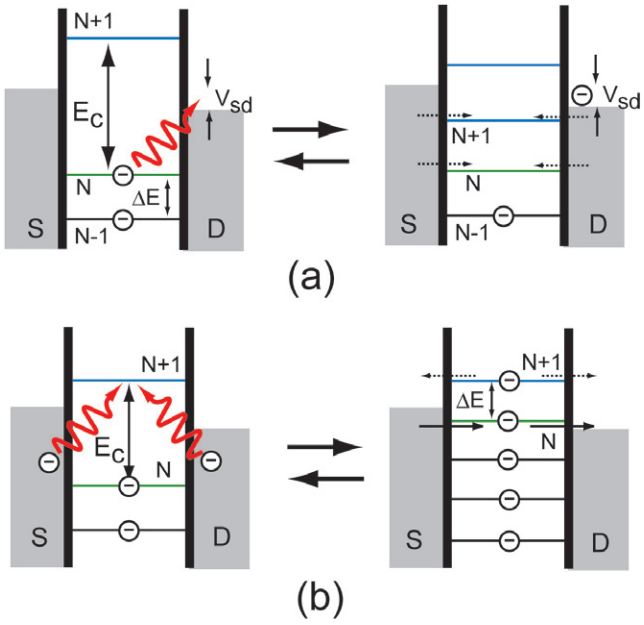

Figure 6. Schematic model of the satellite peaks (a) that move and (b) that do not move as the THz frequency is changed. It should be noted that the peak with the above mechanism (a) should appear on the right-hand side of the main peak, while the peak with the above mechanism (b) should appear on the left-hand side of the main peak.

tunnel barrier has been estimated to be several meV, which is not sufficiently large compared with the THz energy.

Although we have not observed the type-1 peaks, which should move as the THz frequency is changed, on the left-hand side of the main peak, we sometimes observed a satellite peak on this side which did not move as the THz frequency was changed (type-2 peak). Figure 5 shows an example of such a peak with different THz powers. As is shown later, the peak is also photon-related but has a different mechanism to the satellite peaks in figure 4(a) which move with THz frequencies.

An example of such a peak is shown in figure 5 for the fixed THz frequency ($f = 2.5$ THz) and various powers. The peak at $V_g \sim -485$ mV is a main Coulomb peak that appears without THz irradiation. The satellite peak on the left-hand side of the main Coulomb peak does not change its position when the THz frequency is changed (not shown in the figure). The mechanism of the satellite peak is shown in figure 6(b). In this case, an electron in either electrode tunnels into the dot by the THz photon absorption and the Coulomb blockade is lifted. If the energy level of the Nth state, indicated by the green line, happens to come in the bias window set by V_{sd}, the new current channel opens, resulting in the current. When an electron in the source (left electrode) tunnels onto the $N + 1$th level in the dot, followed by tunnelling of the electron in the Nth level out to the drain (right), the process contributes to the current. As soon as the electron in the $N + 1$th level tunnels out to the source or drain electrode, the system comes back to the Coulomb blockade. This process occurs for any THz frequencies if they help an electron tunnel into the dot. Since the necessary condition for the satellite peak is that the Nth level comes in the bias window when the Coulomb blockade is lifted due to the photon absorption, it has nothing to do with THz frequencies. There should be a type-2 peak, which does not move as the THz frequency is changed, on the right-hand side of the main Coulomb peak. But we have not seen it, and do not discuss the mechanism in detail.

For the above THz-PAT processes to be observable, there are some necessary conditions. First, the escape rate (Γ) should be smaller than the THz frequency. For the single-electron

transport, Γ is estimated by the current with $I = e\Gamma$, and is roughly $\sim 10^7$ s^{-1} from the current peak height. Indeed, $\Gamma \ll f$ for the THz waves. Second, E_c should be larger than the corresponding THz frequency. For the sample in figure 4(a), $E_c = 24$ meV is larger than the irradiated THz wave (2.5 THz–10 meV). Third, hf should be larger than the thermal broadening at the electrodes ($\sim k_B T$). At $T = 1.5$ K, $k_B T \ll hf$. These conditions make the THz-PAT possible in the SWCNT-QDs. In the single QD, the temperature ($k_B T$) has to be smaller than hf because of the thermal broadening at the electrodes. This restriction may be removed in the coupled quantum dots where the PAT occurs between the confined levels in each dot [17], the width of which is not determined by the temperature but by the strength of confinement. In this case, the PAT may be observed at much higher temperatures.

The THz power dependence of the peak height is suggestive. The peak height of the main Coulomb peak decreases, while that of the satellite peak increases, as the THz power is increased. These behaviours remind us of the Bessel function behaviour that was first observed in the superconducting tunnel junction irradiated with microwaves [18]. In the SWCNT-QD, the THz field may not directly couple to electrons in the QD since the QD is shielded by the metallic source–drain electrodes with a distance of $\sim$300 nm, which is much smaller than the wavelength of the THz wave. It may couple to the electrodes, so that the V_{sd} oscillates with the THz frequency. V_{sd} is divided into V_s at the source barrier and V_d at the drain barrier, based on resistance at each barrier. Therefore, the tunnelling rate at each barrier, $\Gamma_{S/D}$, may include photon side bands, such that $\Gamma_{S/D} \sim J_n^2(eV_{S/D}/hf)$, where J_n is the nth-order Bessel function. The total current, I, should behave like $I \sim J_n^2(eV_{S/D}/hf)$. This tendency appears to be observed in the main Coulomb peak for $n = 0$ and the satellite peak for $n = 1$ in figure 5.

4. Conclusion

In conclusion, we have fabricated SWCNT-QDs and carried out low temperature transport measurements. It turns out that the SWCNT-QD behaves like an artificial atom, where electrons are confined in the one-dimensional hard wall potential. This is observed as a two- or four-electron periodicity in the Coulomb oscillations. The simple shell structures are realized in the SWCNT because energy scales of electron–electron interactions are much smaller than the level spacings due to quantum confinement. The simple shell structures are also attractive for realization of the spin qubit that can be generated when the number of electrons is odd for the two-electron shell regime.

The energy scales of SWCNT-QDs lie in the THz range, which makes us expect a quantum response to the frequencies. In fact, we have observed the THz photon-assisted tunnelling at a liquid He temperature. This phenomenon could be used for a new type of THz detector with spectroscopic capability.

The characteristics described in this paper arise from the one-dimensional nature of carbon nanotubes (CNT) and may be observed in other one-dimensional systems such as semiconductor nanowires [19]. However, a unique feature of the CNTs may be that the surface of the CNT can be modified chemically, so that the molecular scale nanostructures could be realized.

References

[1] Bockrath M, Cobden D H, McEuen P L, Chopra N G, Zettl A, Thess A and Smalley R E 1997 *Science* **275** 1922
[2] Ishibashi K, Suzuki M, Ida T, Tsukagoshi K and Aoyagi Y 2000 *Japan. J. Appl. Phys.* **39** 7053
[3] Tans S J, Devoret M H, Dai H, Thess A, Smalley R E, Geeligs B L and Dekker C 1997 *Nature* **397** 474
[4] Liang W, Bockrath M and Park H 2002 *Phys. Rev. Lett.* **88** 126801
[5] Moriyama S, Fuse T, Suzuki M, Aoyagi Y and Ishibashi K 2005 *Phys. Rev. Lett.* **94** 186806
[6] Moriyama S, Fuse T, Suzuki M, Aoyagi Y and Ishibashi K 2005 *Appl. Phys. Lett.* **87** 073103
[7] Tarucha S, Austing D G, Honda T, Hage R J vd and Kouwenhiven L P 1996 *Phys. Rev. Lett.* **77** 3613
[8] Fuse T, Kawano Y, Yamaguchi T, Aoyagi Y and Ishibashi K 2007 *Nanotechnology* **18** 044001
[9] Ishibashi K, Moriyama S, Tsuya D, Fuse T and Suzuki M 2006 *J. Vac. Sci. Technol.* A **24** 1349
[10] Loss D and Divincenzo D P 1998 *Phys. Rev.* A **57** 120
[11] Ishibashi K, Moriyama Y and Fuse T 2004 *IEICE Trans. Electron.* **87C** 1799
[12] Beenakker C W J 1991 *Phys. Rev.* B **44** 1646
[13] Averin D V and Likharev K K 1991 *Mesoscopic Phenomena in Solids* ed B Altshuler, P A Lee and R A Webb (Amsterdam: Elsevier) chapter 6
[14] Oreg Y, Byczuk K and Halperin B I 2000 *Phys. Rev. Lett.* **85** 365
[15] Ralph D C, Black C T and Tinkham M 1997 *Phys. Rev. Lett.* **78** 4087
[16] Kawano Y, Fuse T, Toyokawa S, Uchida T and Ishibashi K 2008 Terahertz photon-assisted tunneling in carbon nanotube quantum dots *J. Appl. Phys.* **103** 034307
[17] Oosterkamp T H, Fujisawa T, van der Wiel W G, Ishibashi K, Hijman R V, Tarucha S and Kouwenhoven L P 1998 *Nature* **395** 873
[18] Tien P K and Gordon J P 1963 *Phys. Rev.* **129** 647
[19] Huang S, Fukata N, Shimizu M, Yamaguchi T, Sekiguchi T and Ishibashi K 2008 *Appl. Phys. Lett.* **92** 213110